IEEE Access
Multidisciplinary | Rapid Review | Open Access Journal

Received June 29, 2021, accepted July 12, 2021, date of publication July 26, 2021, date of current version July 30, 2021.

Digital Object Identifier 10.1109/ACCESS.2021.3099216

An Ultra-Wideband Circular Polarization-Maintaining Metasurface and Its Application in RCS Reduction

BAOQIN LIN, (Member, IEEE), WENZHUN HUANG, LINTAO LV, JIANXIN GUO, ZHE LIU, AND RUI ZHU
School of Information Engineering, Xijing University, Xi'an, Shaanxi 710123, China

Corresponding author: Baoqin Lin (aflbq@sina.com)

This work was supported in part by the National Natural Science Foundation of China under Grant 62072378, in part by the Natural Science Foundation of Shaanxi Province, China, under Grant 2019JM-077, and in part by the Xi'an Science and Technology Plan Project, China, under Grant GXYD20.4.

ABSTRACT In this work, a circular polarized (CP) maintaining metasurface is proposed, which can realize ultra-wideband CP-maintaining reflection and make its co-polarization reflection coefficient under CP incidence close to 1.0 in the frequency band 6.2-26.4GHz; in addition, by rotating its unit cell structure, Pancharatnam-Berry (PB) phase can be generated in its co-polarized reflection coefficient under CP incidence. Thus based on the CP-maintaining metasurface, a 2-bit PB coding metasurface is further proposed for Radar Cross Section (RCS) reduction. The simulated results show that the proposed PB coding metasurface has excellent performance in RCS reduction, compared with a pure metal plate with the same size, its RCS can be reduced more than10dB under arbitrary polarization incidences in the frequency band 6.2-26.5GHz with relative band of 124.1%. Finally, an effective experimental validation is carried out.

INDEX TERMS Pancharatnam-berry (PB) phase, coding metasurface, radar cross section (RCS).

I. INTRODUCTION

Polarization is one of important properties of electromagnetic(EM) wave, which must be taken into consideration in most practical applications. To manipulate it freely, polarization converter has been a kind of widely used device. Conventional polarization converters were usually designed by using the birefringence effect and optical activity of natural materials, which often suffer from bulky volume, high loss, and narrow bandwidth in practical applications [1], [2]. Over the past decade, it has been found that metasurface can provide a convenient way to control the polarization state of EM wave. In recent years, to update the conventional design method, many different types of polarization converters have been proposed based on various anisotropic or chiral metasurfaces, which can perform different polarization conversions, such as cross [3]–[10] or linear-to-circular [11]–[17] polarization conversion. In addition, A right-handed/left-handed circularly polarized (RCP/ LCP) wave will be converted to a LCP/ RCP one after reflection on a conducting surface, however, based on a proper anisotropic or chiral metasurface, a CP-maintaining metasurface can be proposed, which can keep the handedness of the reflected wave the same as that of the CP incident one. [18]–[21] This kind of CP-maintaining metasurface can be regarded as a reflective circular polarization converter, [21] which is very useful in the design of reflective Pancharatnam-Berry (PB) gradient metasurfaces [22]–[27] and PB coding metasurfaces [28]–[32] because PB phase can only be generated in the co-polarized reflected wave under CP incidence for a reflective metasurface. [33] The concept of coding metasurface was firstly proposed by Cui *et al.* [34] which consisted of several different types of elements arranged as a predesigned coding sequence. It can work as a reflective phased array antenna, its far-field scattering pattern can be controlled by the predesigned coding sequence, so it can achieve Radar Cross Section (RCS) reduction by optimizing the coding sequence. In recent years, to realize wideband RCS reduction, a number of different coding metasurfaces have been proposed [35]–[41].

The associate editor coordinating the review of this manuscript and approving it for publication was Xinxing Zhou.

In this work, an ultra-wideband CP-maintaining metasurface is proposed, which is an orthogonal anisotropic structure with a pair of symmetric axes. The simulated results show that the proposed metasurface can realize ultra-wideband CP-maintaining reflection in the frequency band 6.2-26.4 GHz; moreover, if the notched circular metal patch in its unit cell is rotated by an angle ψ, almost $\pm 2\psi$ PB phase will be generated in its co-polarized reflection coefficient under CP incidence, when the rotating angle is chosen as 0°, 45°, 90° and 135°, it can be used as 2-dit coding elements "00", "01", "10" and "11", respectively. Thus, based on the CP-maintaining metasurface, an ultra-wideband 2-bit PB coding metasurface is further proposed for RCS reduction.

II. DESIGN AND SIMULATION

The proposed CP-maintaining metasurface consists of a notched circular metal patch array printed on a grounded dielectric substrate and covered by a dielectric layer. One of its unit cells is shown in Fig. 1, it is indicated that the unit cell structure is symmetric with respect to both x and y axes. In addition, the geometrical parameters of the unit cell structure are shown in Fig. 1. Through the optimization of HFSS software, the geometrical parameters have been selected as follows: $P = 6.00$ mm, $r = 2.80$ mm, $w = 0.45$ mm, $g = 2.60$ mm, $h_1 = 2.20$ mm and $h_2 = 2.70$ mm; in addition, the circular metal patch, together with the grounded plane, is modeled as a 0.017mm copper film with an electric conductivity $\sigma = 5.8 \times 10^7$ S/m, and the two dielectric layers are chosen as a F4B-2 with relative permittivity of 2.65.

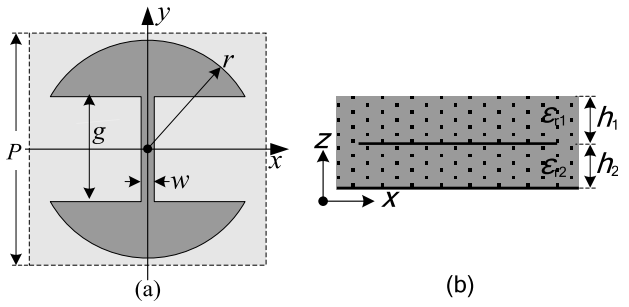

FIGURE 1. Unit cell of the proposed CP-maintaining metasurface: (a) Top view (b) Side view.

When the proposed CP-maintaining metasurface is under x-polarized (XP) and y-polarized (YP) incidences, no cross-polarized components will exist in the reflected wave due to the symmetry of the metasurface structure, [6] thus its reflection matrix $\mathbf{R}_{\mathrm{Lin}}$ for linear-polarized (LP) wave can be expressed as:

$$\mathbf{R}_{\mathrm{Lin}} = \begin{pmatrix} r_{xx} & 0 \\ 0 & r_{yy} \end{pmatrix}. \tag{1}$$

The magnitudes of r_{xx} and r_{yy} will both be close to 1.0 because the dielectric loss is very little, and the following formula can be established when the little dielectric loss is neglected:

$$r_{yy} = r_{xx} e^{-j\Delta\varphi_{xy}}, \tag{2}$$

wherein $\Delta\varphi_{xy}$ denotes the phase difference between r_{xx} and r_{yy}. Thus when the incident wave is assumed as a CP one $\boldsymbol{E}_i = E_0(\hat{e}_x \pm i\hat{e}_y)$, based on Eq. (1) and (2), the reflection matrix $\mathbf{R}_{\mathrm{Cir}}$ for CP wave can be obtained as follow [25]:

$$\begin{aligned} \mathbf{R}_{\mathrm{Cir}} &= \begin{pmatrix} r_{++} & r_{+-} \\ r_{-+} & r_{--} \end{pmatrix} = \frac{1}{2}\begin{pmatrix} r_{xx} - r_{yy} & r_{xx} + r_{yy} \\ r_{xx} + r_{yy} & r_{xx} - r_{yy} \end{pmatrix} \\ &= \frac{1}{2} r_{xx} \begin{pmatrix} 1 + e^{-j\Delta\varphi} & 1 - e^{-j\Delta\varphi} \\ 1 - e^{-j\Delta\varphi} & 1 + e^{-j\Delta\varphi} \end{pmatrix}. \end{aligned} \tag{3}$$

Based on Eq. (3), the magnitudes of co- and cross-polarized reflection coefficients r_{++}, r_{--} and r_{-+}, r_{+-} can be expressed as:

$$\begin{aligned} |r_{++}| = |r_{--}| &= \frac{1}{2}|r_{xx}|\left|1 - e^{-j\Delta\varphi_{xy}}\right| = \sqrt{(1 - \cos\Delta\varphi_{xy})/2} \\ |r_{-+}| = |r_{+-}| &= \frac{1}{2}|r_{xx}|\left|1 + e^{-j\Delta\varphi_{xy}}\right| = \sqrt{(1 + \cos\Delta\varphi_{xy})/2}. \end{aligned} \tag{4}$$

Eq. (4) indicates that the polarization state of the reflected wave under CP incidence can be completely determined by the phase difference $\Delta\varphi_{xy}$ between r_{xx} and r_{yy}, if the phase difference $|\Delta\varphi_{xy}|$ is equal to 180°, a perfect CP-maintaining reflection ($|r_{-+}| = |r_{-+}| = 0, |r_{++}| = |r_{--}| = 1$) can be realized. Why the perfect CP-maintaining reflection can be realized when $|\Delta\varphi_{xy}| = 180°$? In fact, when the little dielectric loss of the metasurface is neglected, the CP incident wave and the reflected wave of the metasurface can both be regarded as a composite wave composed of XP and YP components with equal amplitudes. The two components in the CP incident wave are with ±90° phase difference, however, in the reflected wave, the phase difference will be changed. When $|\Delta\varphi_{xy}| = 180°$, ±90° phase difference in the CP incident wave will be changed as ∓90° in the reflected wave, thus the perfect CP-maintaining reflection will be realized.

Can the proposed metasurface realize CP-maintaining reflection? To numerically analyze the performance of the proposed metasurface, we have first simulated it under XP and YP incidences using Ansoft HFSS. The simulated results, the phase difference $\Delta\varphi_{xy}$ between r_{xx} and r_{yy}, are shown in Fig. 2(a), it is indicated that the phase difference $\Delta\varphi_{xy}$ is close to 180° in the ultra-wide frequency band from 7 to 26 GHz, which implies that the anticipated CP-maintaining reflection can be realized in the frequency band. To show it, the magnitudes of r_{++} and r_{-+} have been calculated by using Eq. (4) according to the phase differences $\Delta\varphi_{xy}$ in Fig. 2(a), the calculated results, shown in Fig. 2(b), indicate that the magnitude of r_{++} is approximate to 0dB, however, that of r_{-+} is kept less than -10dB in the frequency band from 6.2 to 26.4 GHz, which shows that the anticipated CP-maintaining reflection will be realized under CP incidence, and the relative bandwidth reachs up to 123.9%. Furthermore, in order to

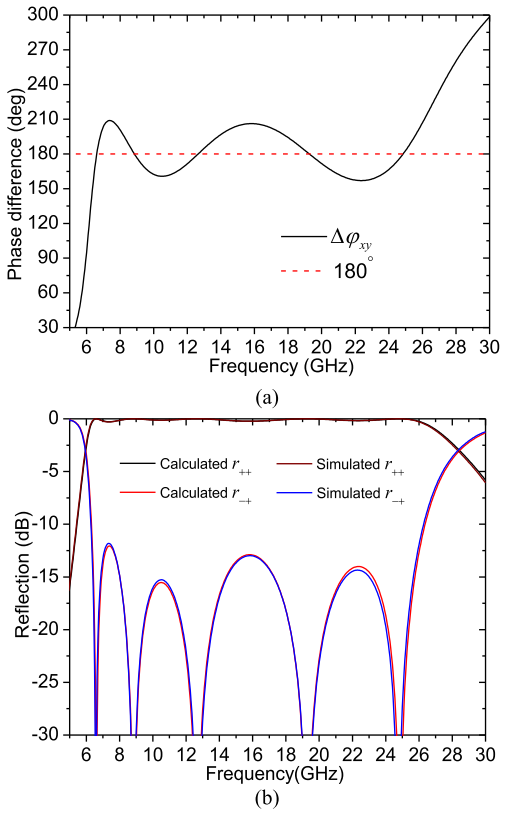

FIGURE 2. Simulated results of the proposed CP-maintaining metasurface: (a) the phase difference between r_{xx} and r_{yy} (b) the magnitudes of r_{++} and r_{-+}.

verify the correctness of the calculated results, the metasurface has been simulated under RCP incidence. The simulated results are also shown in Fig. 2(b), it is indicated that the calculated and simulated results are in good agreement with each other.

Moreover, will there be PB phase generated in the co-polarization reflection coefficients r_{++} and r_{--} by rotating the circular metal patch in the unit cell of the CP-maintaining metasurface? In fact, when the circular metal patch is rotated by an angle ψ in anticlockwise direction, the reflection matrix $\mathbf{R}_{\mathrm{Lin}}$ for LP wave will be changed, thus the reflection matrix $\mathbf{R}_{\mathrm{Cir}}$ for CP wave obtained based on $\mathbf{R}_{\mathrm{Lin}}$ will also be changed, and the components of the changed $\mathbf{R}_{\mathrm{Cir}}$ can be expressed as follows [26]:

$$\begin{aligned} r_{++} &= \frac{1}{2}\left(r_{xx} - r_{yy}\right) e^{+\mathrm{j}2\psi} \\ r_{--} &= \frac{1}{2}\left(r_{xx} - r_{yy}\right) e^{-\mathrm{j}2\psi} \\ r_{+-} &= \frac{1}{2}\left(r_{xx} + r_{yy}\right) \\ r_{-+} &= \frac{1}{2}\left(r_{xx} + r_{yy}\right). \end{aligned} \tag{5}$$

Eq. (5) illustrates that when the circular metal patch is rotated by an angle, the PB phases generated in the co-polarization reflection coefficients r_{++} and r_{--} will be $+2\psi$ and -2ψ respectively, however, the phases of r_{+-} and r_{-+} will not be changed.

To verify the theoretical prediction, the CP-maintaining metasurface has been simulated under RCP and LCP normal incidences when the rotation angle ψ of the circular metal patch in its unit cell was gradually increased from 0° to 180° with a 22.5° step width. The simulated results, shown in Fig. 3(a) and (b), indicate that the phase of r_{++} keeps increasing gradually but the phase of r_{--} keeps decreasing gradually along with the increase of the rotation angle at the five frequencies 8, 12, 16, 20 and 24 GHz, and they are both altered by almost 45° at each time, which verifies that when the circular metal patch in the unit cell of the CP-maintaining metasurface is rotated by ψ, the PB phases generated in the co-polarized reflection coefficients r_{++} and r_{--} are almost $+2\psi$ and -2ψ, respectively.

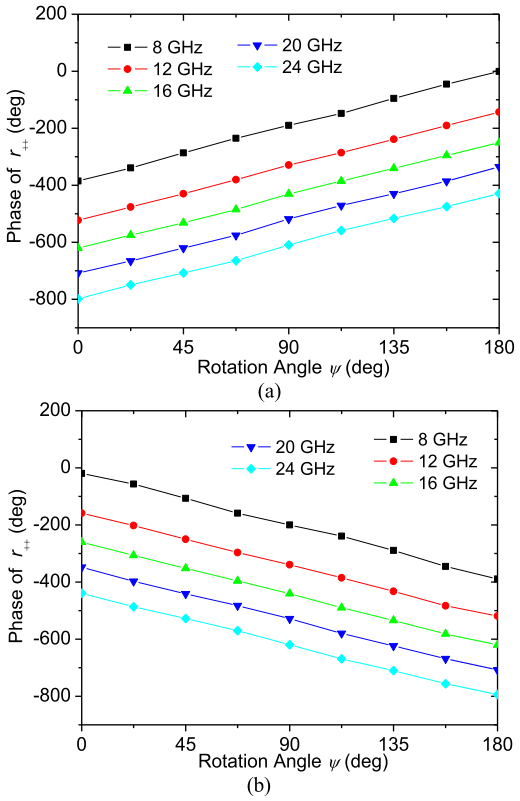

FIGURE 3. Simulated results of the CP-maintaining metasurface with different rotating angle ψ: (a) the phase of r_{++}, (b) the phase of r_{--}.

III. APPLICATION IN RCS REDUCTION

The above simulations show that the proposed metasurface can realize ultra-wideband CP-maintaining reflection in the frequency range from 6.2 to 26.4 GHz; moreover, PB phase will be generated in r_{++} and r_{--} by rotating the circular metal patch in its unit cell. Thus, the proposed metasurface can be used in the design of coding metasurface.

To design a 2-bit coding metasurface for RCS reduction, we construct four basic coding sub-unit cells at first by using

the unit cell of the proposed CP-maintaining metasurface, they are shown in Fig. 4(a), in which the circular metal patches have been rotated by 0°, 45°, 90° and 135° respectively. According to the simulated results shown in Fig. 3, it is known that the relative reflection phases of the four basic coding sub-unit cells will be 0°, 90°, 180° and 270° respectively under RCP incidence, so their codes shall be "00", "01", "10" and "11"; however, under LCP incidence, their codes shall be changed as "11", "10", "01" and "00" respectively because the PB phases generated in r_{++} and r_{--} are opposite. In the following, the design is carried out under RCP incidence, the codes of the four basic coding sub-unit cells will be defined relative to RCP incident wave. Secondly, when the designed 2-bit coding metasurface is assumed to consist of 6 × 6 coding elements, and each digital element is composed of 5 × 5 identical basic sub-unit cells, one optimized coding sequence is obtained through the optimization of genetic algorithm aiming at minimizing scattering in all directions. Thus, according to the optimized coding sequence, one appropriate 2-bit coding metasurface is proposed, which is shown in Fig. 4(b). For the proposed 2-bit coding metasurface, the reflection amplitudes in various digital elements are basically the same, but the reflection phases are different. The reflection phase differences between "00" and "10" and between "01" and "11" will both be close to 180° under RCP incidence, in addition, under LCP incidence, these phase differences will be close to −180°, so the best RCS reduction can be realized under arbitrary polarization incidences due to phase cancellation because these coding elements are arranged according to the optimized coding sequence.

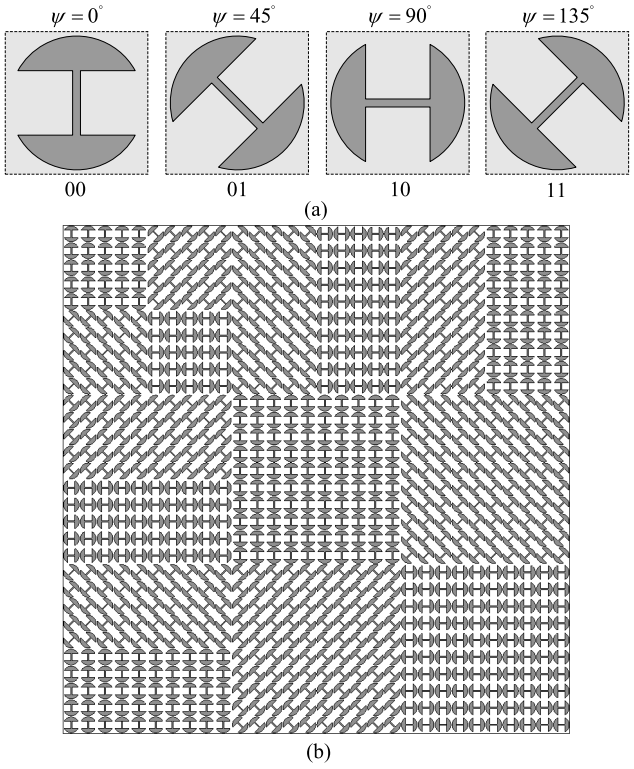

FIGURE 4. (a) Four basic sub-unit cells (b) Layout of the proposed 2-bit coding metasurface.

To verify the performance of the 2-bit coding metasurface, a series of numerical simulations have been carried out by using CST Microwave Studio. Firstly, the 2-bit coding metasurface, together with a pure metal plate with the same size, was simulated under RCP, LCP, XP and YP normal incidences successively. The simulated results, the monostatic RCSs of the coding metasurface and the metal plate, are shown in Fig. 5(a); in addition, the RCS reduction of the coding metasurface relative to the metal plate is shown in Fig. 5(b). In Fig. 5, it is indicated that the RCS of the coding metasurface is almost the same under different polarization incidences; in addition, relative to the metal plate, the RCS of the coding metasurface is reduced more than 10dB under all incidences in the ultra-wide frequency band from 6.2 to 26.5 GHz with relative bandwith of 124.1%, and the maximum reduction can reach 33.8dB, 34.1dB, 36.6dB and 34.9dB respectively under RCP, LCP, XP and YP normal incidences at 19.4GHz.

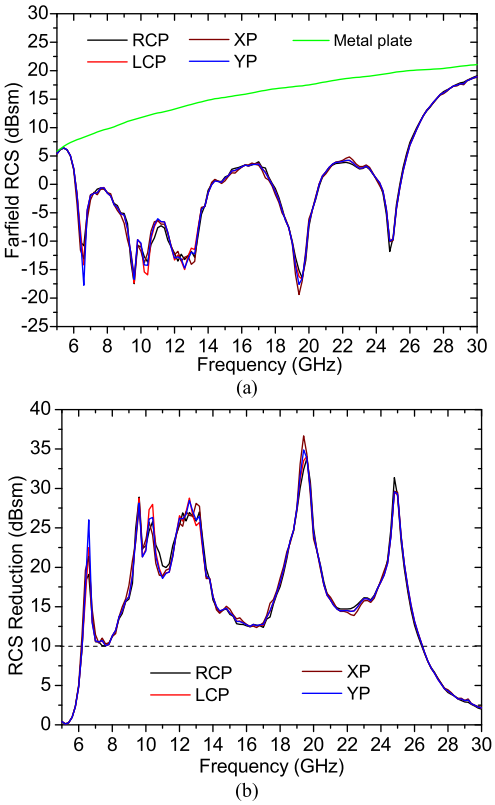

FIGURE 5. Simulated results of the coding metasurface and the metal plate: (a) the monostatic RCS, (b) the RCS reduction of the coding metasurface.

In addition, to show far-field scattering characteristics of the coding metasurface, the far-field scattering patterns of the coding metasurfaces and the pure metal plate with same size have been simulated under LCP, RCP, XP and YP normal incidences at 8.0, 16.0 and 24.0 GHz. The simulated results,

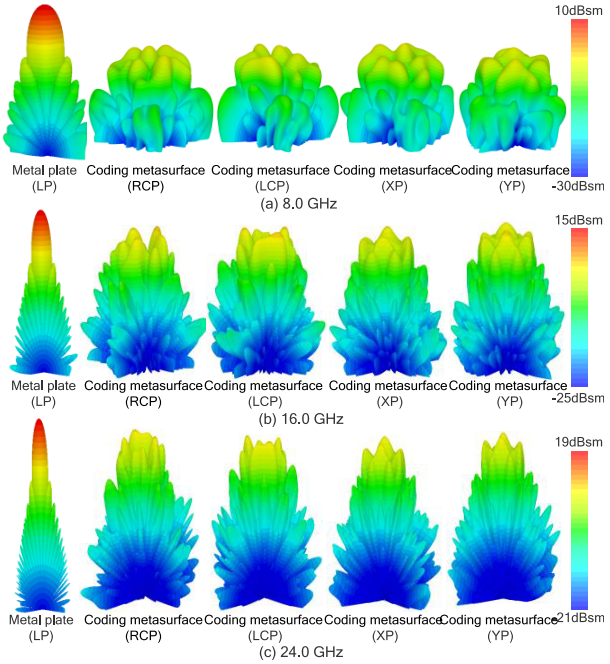

FIGURE 6. Simulated 3D far-field scattering patterns of the proposed coding metasurface and the metal plate under LCP, RCP, XP and YP normal incidences at (a) 8.0 GHz, (b) 16.0 GHz and (c) 24.0 GHz.

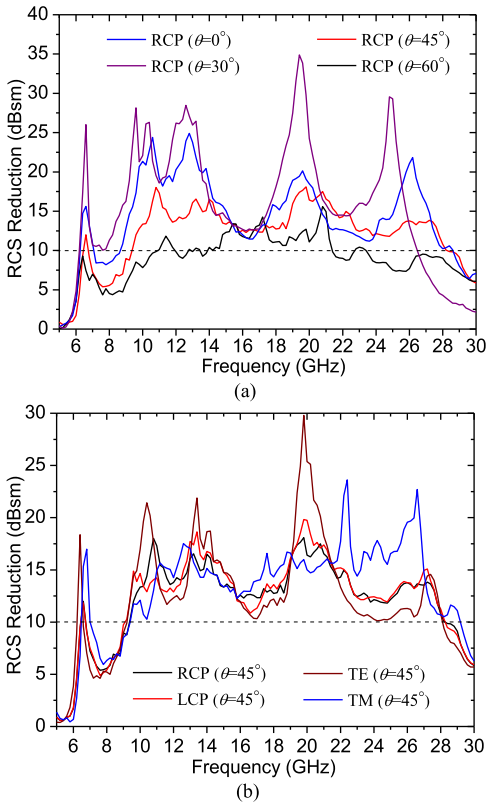

FIGURE 7. RCS reduction of the coding metasurface under different oblique incidences: (a) RCP incidence with different incident angles; (b) different polarization incidences with incident angle of 45°.

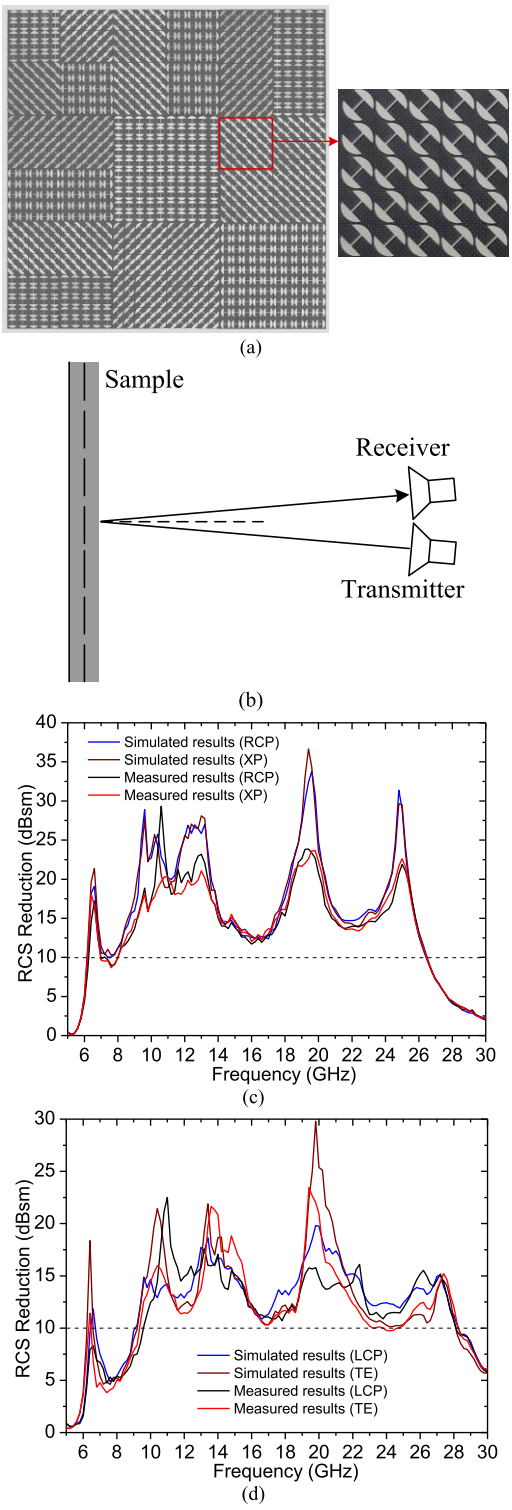

FIGURE 8. Photographs of the fabricated laboratory sample (a), the schematic of the measurement setup (b) and the comparison between measured and simulated results under normal incidences (c) and under oblique incidences with incident angle of 45° (d).

shown in Fig. 6, indicate that when the coding metasurface is under LCP, RCP, XP and YP normal incidences, its far-field scattering characteristics are basically the same, compared with the strong specular reflection of the pure metal plate, its reflected wave has been scatterd in all directions of the specular reflection region, so the coding metasurface can realize

ultra-wideband RCS reduction under arbitrary polarization incidences.

Furthermore, to analyse the angle insensitivity, the 2-dit PB coding metasurface has been simulated under different oblique incidences, the simulated results are shown in Fig. 7. In Fig. 7(a), it is indicated that when the incident angle increases to 45°, the monostatic RCS reduction of the coding metasurface is still kept larger than 10dB in the ultra-wide frequency band 9.4-28.3GHz under RCP incidence; especially, when the incident angle is as high as 60°, the RCS reduction can still be close to 10dB in the band. In addition, Fig. 7(b) indicates that the RCS reduction is roughly the same under different polarization incidences with incident angle of 45°. According to these simulated results, it is known that the coding metasurface has good angular stability under arbitrary polarization incidences.

Finally, to carry out an experimental verification for the 2-bit coding metasurface, one laboratory sample has been fabricated. In the fabricating process, the grounded dielectric substrate was fabricated by PCB technology, which is shown in Fig. 8(a), and the whole structure was obtained by hot pressing it with the top dielectric layer. The laboratory sample, together with a pure metal plate with the same size, has been measured under normal incidence and oblique incidence with incident angle of 45°. The schematic illustration of the measurement setup is shown in Fig. 8(b), in which a pair of identical horn antennas as transmitter and receiver have been connected to the two ports of an Agilent E8363B network analyzer, and the sample was irradiated; for oblique incidence, the separation angle between the orientations of the pair of antennas was chosen as 90°, however, for normal incidence, the separation angle should be equal to 0°, it was set to be 5° for the finite sizes of the laboratory sample. The measured results under RCP, XP normal incidences and LCP, TE oblique incidences are shown in Fig. 8(c) and (d) respectively, it is indicated that the measured results are all in reasonable agreement with the simulated results except for a slight deviation caused by fabrication and measurement errors.

IV. CONCLUSION

In this work, an ultra-wideband reflective 2-bit PB coding metasurface was proposed for RCS resdution. In the design process, a CP-maintaining metasurface was proposed firstly, which can realize ultra-wideband CP-maintaining reflection in the frequency band 6.2-26.4GHz, moreover, PB phase will be generated in its co-polarization reflection coefficient under CP incidence by rotating the circular metal patch in its unit cell. Thus the ultra-wideband 2-bit PB coding metasurface was proposed based on the CP-maintaining metasurface. The simulated and measured results show that compared with a pure metal plate with the same size, the RCS of the coding metasurface under normal incidence with arbitrary polarization can be reduced more than 10 dB in the frequency band 6.2-26.5 GHz with relative bandwith of 124.1%; in addition, when the incident angle is up to 45°, the RCS reduction is still kept larger than 10dB in the band 9.4-28.3GHz. Table 1 lists the comparison of the coding metasurface with previous works presented in [35]–[41] it is indicated that the coding metasurface can achieve much wider band RCS reduction, so it has great potential in radar stealth technology application.

TABLE 1. Comparison of this work with previous works.

Ref.	RCS Redution(dB)	Freq. Band(GHz)	FBW	Max RCS Redution(dB)
[35]	10	17-42	84.7%	24
[36]	10	12.2-23.4	62.9%	25.2
[37]	10	15.4-29.3	62.2%	29
[38]	10	3.90-4.05	3.8%	18
[39]	10	15-40	91%	18.8
[40]	10	15-35	80%	36
[41]	10	6.94-9.23	28.3%	35.5
This work	10	6.2-26.5	124.1%	36.6

REFERENCES

[1] L. Young, L. A. Robinson, and C. Hacking, "Meander-line polarizer," *IEEE Trans. Antennas Propag.*, vol. 21, no. 3, pp. 376–378, May 1973.

[2] Y. Huang, Y. Zhou, and S.-T. Wu, "Broadband circular polarizer using stacked chiral polymer films," *Opt. Exp.*, vol. 15, no. 10, p. 6414, 2007.

[3] X. Gao, X. Han, W.-P. Cao, H. O. Li, H. F. Ma, and T. J. Cui, "Ultrawideband and high-efficiency linear polarization converter based on double V-shaped metasurface," *IEEE Trans. Antennas Propag.*, vol. 63, no. 8, pp. 3522–3530, Aug. 2015.

[4] Y. Jia, Y. Liu, Y. J. Guo, K. Li, and S.-X. Gong, "Broadband polarization rotation reflective surfaces and their applications to RCS reduction," *IEEE Trans. Antennas Propag.*, vol. 64, no. 1, pp. 179–188, Jan. 2016.

[5] B. Lin, B. Wang, W. Meng, X. Da, W. Li, Y. Fang, and Z. Zhu, "Dual-band high-efficiency polarization converter using an anisotropic metasurface," *J. Appl. Phys.*, vol. 119, no. 18, 2016, Art. no. 205428.

[6] B. Q. Lin, X. Y. Da, J. L. Wu, W. Li, Y. W. Fang, and Z. H. Zhu, "Ultra-wideband and high-efficiency cross polarization converter based on anisotropic metasurface," *Miceow. Opt. Tech. Lett.*, vol. 58, no. 10, pp. 2402–2405, Oct. 2016.

[7] Z. L. Mei, X. M. Ma, C. Lu, and Y. D. Zhao, "High-efficiency and wide-bandwidth linear polarization converter based on double U-shaped metasurface," *AIP Adv.*, vol. 7, no. 12, Dec. 2017, Art. no. 125323.

[8] M. I. Khan, Q. Fraz, and F. A. Tahir, "Ultra-wideband cross polarization conversion metasurface insensitive to incidence angle," *J. Appl. Phys.*, vol. 121, no. 4, Jan. 2017, Art. no. 045103.

[9] X. Jin, R. Li, J. Qin, S. Wang, and T. Han, "Ultra-broadband wide-angle linear polarization converter based on H-shaped metasurface," *Opt. Exp.*, vol. 26, no. 16, pp. 20913–20919, 2018.

[10] Y. Zhao, B. Qi, T. Niu, Z. Mei, L. Qiao, and Y. Zhao, "Ultra-wideband and wide-angle polarization rotator based on double W-shaped metasurface," *AIP Adv.*, vol. 9, no. 8, Aug. 2019, Art. no. 085013.

[11] E. Doumanis, G. Goussetis, J. L. Gomez-Tornero, R. Cahill, and V. Fusco, "Anisotropic impedance surfaces for linear to circular polarization conversion," *IEEE Trans. Antennas Propag.*, vol. 60, no. 1, pp. 212–219, Jan. 2012.

[12] H. L. Zhu, S. W. Cheung, K. L. Chung, and T. I. Yuk, "Linear-to-circular polarization conversion using metasurface," *IEEE Trans. Antennas Propag.*, vol. 61, no. 9, pp. 4615–4623, Sep. 2013.
[13] Y. Jiang, L. Wang, J. Wang, C. N. Akwuruoha, and W. Cao, "Ultra-wideband high-efficiency reflective linear-to-circular polarization converter based on metasurface at terahertz frequencies," *Opt. Exp.*, vol. 25, no. 22, pp. 27616–27623, 2017.
[14] J. D. Baena, S. B. Glybovski, J. P. del Risco, A. P. Slobozhanyuk, and P. A. Belov, "Broadband and thin linear-to-circular polarizers based on self-complementary zigzag metasurfaces," *IEEE Trans. Antennas Propag.*, vol. 65, no. 8, pp. 4124–4133, Aug. 2017.
[15] S. Sun, W. Jiang, S. Gong, and T. Hong, "Reconfigurable linear-to-linear polarization conversion metasurface based on PIN diodes," *IEEE Antennas Wireless Propag. Lett.*, vol. 17, no. 9, pp. 1722–1726, Sep. 2018.
[16] H.-F. Zhang, L. Zeng, G.-B. Liu, and T. Huang, "Tunable linear-to-circular polarization converter using the graphene transmissive metasurface," *IEEE Access*, vol. 7, pp. 158634–158642, 2019.
[17] B. Lin, L. Lv, J. Guo, Z. Liu, X. Ji, and J. Wu, "An ultra-wideband reflective linear-to-circular polarization converter based on anisotropic metasurface," *IEEE Access*, vol. 8, pp. 82732–82740, 2020.
[18] Y.-F. Li, J.-Q. Zhang, S.-B. Qu, J.-F. Wang, L. Zheng, H. Zhou, Z. Xu, and A.-X. Zhang, "Wide-band circular polarization-keeping reflection mediated by metasurface," *Chin. Phys. B*, vol. 24, no. 1, pp. 258–264, 2015.
[19] J. Yang, S. Qu, H. Ma, J. Wang, S. Sui, Q. Zheng, H. Chen, and Y. Pang, "Ultra-broadband co-polarization anomalous reflection metasurface," *Appl. Phys. A, Solids Surf.*, vol. 123, no. 8, p. 537, Aug. 2017.
[20] B. Lin, J. Guo, L. Lv, J. Wu, Y. Ma, B. Liu, and Z. Wang, "Ultra-wideband and high-efficiency reflective polarization converter for both linear and circular polarized waves," *Appl. Phys. A, Solids Surf.*, vol. 125, no. 2, p. 76, 2019.
[21] X. Huang, J. Chen, and H. Yang, "High-efficiency wideband reflection polarization conversion metasurface for circularly polarized waves," *J. Appl. Phys.*, vol. 122, no. 4, Jul. 2017, Art. no. 043102.
[22] H.-X. Xu, G.-M. Wang, T. Cai, J. Xiao, and Y.-Q. Zhuang, "Tunable Pancharatnam–Berry metasurface for dynamical and high-efficiency anomalous reflection," *Opt. Exp.*, vol. 24, no. 24, pp. 27836–27848, 2016.
[23] Y. Ran, J. Liang, T. Cai, and H. Li, "High-performance broadband vortex beam generator using reflective Pancharatnam–Berry metasurface," *Opt. Commun.*, vol. 427, pp. 101–106, Nov. 2018.
[24] H. X. Xu, H. Liu, X. Ling, Y. Sun, and F. Yuan, "Broadband vortex beam generation using multimode Pancharatnam–Berry metasurface," *IEEE Trans. Antennas Propag.*, vol. 65, no. 12, pp. 7378–7382, Dec. 2017.
[25] B. Lin, J. Guo, L. Lv, Z. Liu, X. Ji, and J. Wu, "An ultra-wideband reflective phase gradient metasurface using Pancharatnam–Berry phase," *IEEE Access*, vol. 7, pp. 13317–13325, 2019.
[26] B. Lin, L. Lv, J. Guo, Z. Wang, and S. Huang, "Ultra-wideband anomalous reflection realised by a gradient metasurface," *IET Microw., Antennas Propag.*, vol. 14, no. 12, pp. 1424–1430, 2020.
[27] Y. Ran, T. Cai, L. Shi, J. Wang, J. Liang, S. Wu, J. Li, and Y. Liu, "High-performance transmissive broadband vortex beam generator based on Pancharatnam–Berry metasurface," *IEEE Access*, vol. 8, pp. 111802–111810, 2020.
[28] Q. Zheng, Y. Li, J. Zhang, H. Ma, J. Wang, Y. Pang, Y. Han, S. Sui, Y. Shen, H. Chen, and S. Qu, "Wideband, wide-angle coding phase gradient metasurfaces based on Pancharatnam–Berry phase," *Sci. Rep.*, vol. 7, no. 1, p. 43543, Apr. 2017.
[29] J. Li and J. Yao, "Manipulation of terahertz wave using coding Pancharatnam–Berry phase metasurface," *IEEE Photon. J.*, vol. 10, no. 5, Oct. 2018, Art. no. 5900512.
[30] T. Zhao, X. Jing, X. Tang, X. Bie, T. Luo, H. Gan, Y. He, C. Li, and Z. Hong, "Manipulation of wave scattering by Fourier convolution operations with Pancharatnam–Berry coding metasurface," *Opt. Lasers Eng.*, vol. 141, Jun. 2021, Art. no. 106556.
[31] S. J. Li, Y. Li, R. Li, Q. Cheng, and T. Cui, "Digital-coding-feeding metasurfaces for differently polarized wave emission, orbit angular momentum generation, and scattering manipulation," *Adv. Photon. Res.*, vol. 1, Nov. 2020, Art. no. 2000012.
[32] Y. Tian, X. Jing, H. Yu, H. Gan, C. Li, and Z. Hong, "Manipulation of the arbitrary scattering angle based on all-dielectric transmissive Pancharatnam Berry phase coding metasurfaces in the visible range," *Opt. Exp.*, vol. 28, no. 21, pp. 32107–32123, 2020.
[33] S. Pancharatnam, "Generalized theory of interference and its applications," *Proc. Indian Acad. Sci. A*, vol. 44, no. 6, pp. 398–417, 1956.
[34] T. J. Cui, M. Q. Qi, X. Wan, J. Zhao, and Q. Cheng, "Coding metamaterials, digital metamaterials and programmable metamaterials," *Light: Sci. Appl.*, vol. 3, no. 10, p. e218, Oct. 2014.
[35] H. Sun, C. Gu, X. Chen, Z. Li, L. Liu, B. Xu, and Z. Zhou, "Broadband and broad-angle polarization-independent metasurface for radar cross section reduction," *Sci. Rep.*, vol. 7, no. 1, Feb. 2017, Art. no. 407821.
[36] F. Yuan, G.-M. Wang, H.-X. Xu, T. Cai, X.-J. Zou, and Z.-H. Pang, "Broadband RCS reduction based on spiral-coded metasurface," *IEEE Antennas Wireless Propag. Lett.*, vol. 16, pp. 3188–3191, 2017.
[37] M. Feng, Y. Li, Q. Zheng, J. Zhang, Y. Han, J. Wang, H. Chen, S. Sai, H. Ma, and S. Qu, "Two-dimensional coding phase gradient metasurface for RCS reduction," *J. Phys. D, Appl. Phys.*, vol. 51, no. 37, Sep. 2018, Art. no. 375103.
[38] L. Shao, M. Premaratne, and W. Zhu, "Dual-functional coding metasurfaces made of anisotropic all-dielectric resonators," *IEEE Access*, vol. 7, pp. 45716–45722, 2019.
[39] Y. Saifullah, A. B. Waqas, G.-M. Yang, F. Zhang, and F. Xu, "4-bit optimized coding metasurface for wideband RCS reduction," *IEEE Access*, vol. 7, pp. 122378–122386, 2019.
[40] H. Hao, S. Du, and T. Zhang, "Small-size broadband coding metasurface for RCS reduction based on particle swarm optimization algorithm," *Prog. Electromagn. Res. M*, vol. 81, pp. 97–105, 2019.
[41] X. Han, H. Xu, Y. Chang, M. Lin, Z. Wenyuan, X. Wu, and X. Wei, "Multiple diffuse coding metasurface of independent polarization for RCS reduction," *IEEE Access*, vol. 8, pp. 162313–162321, 2020.

BAOQIN LIN (Member, IEEE) received the M.Sc. degree in electromagnetic field and microwave technology from Air Force Engineering University, Xi'an, China, in 2002, and the Ph.D. degree in electronic science and technology from the National University of Defense Technology, Changsha, China, in 2006. He is currently an Associate Professor with the Department of Information Engineering, Xijing University, Xi'an. His current research interests include metasurface for various applications, such as polarization conversion, coupling suppression and RCS reduction, phased-array antennas, and ultra-wideband antennas. He is a member of IEEE Antennas and Propagation Society.

WENZHUN HUANG received the M.Sc. degree in communication and information systems from Air Force Engineering University, Xi'an, China, in 1997, and the Ph.D. degree in information and communications engineering from Northwest Polytechnic University, Xi'an, in 2010. He has been published over 50 academic articles. He is currently a Full Professor and also a Doctor Advisor with the Internet of Things and Big Data Technology Research Center, Xijing University, Xi'an. His research interests include information processing, big data, wireless communication systems, and the IoT technology. He is a member of the Institute of Electronics, Information and Communication Engineers (IEICE).

LINTAO LV received the M.Sc. degree in computer science and technology from Xi'an Jiaotong University, Xi'an, China, in 1982. He is currently a Full Professor and also a Doctor Advisor with the Department of Information Engineering, Xijing University, Xi'an. He has published over 90 journal and international conference papers. His current research interests include artificial intelligence in big data, intelligent information processing, biological information security, pattern recognition, and cyber analysis and security.

JIANXIN GUO received the M.Sc. degree in information and communications engineering from Air Force Engineering University, Xi'an, China, in 2000, and the Ph.D. degree in information and communications engineering from PLA Information Engineering University, Zhengzhou, China, in 2004. He is currently a Professor with the Department of Information Engineering, Xijing University, Xi'an. His current research interests include cognitive radio technologies and MIMO–OFDM wireless communications and their implementation in GNU radio.

ZHE LIU received the Ph.D. degree in control engineering and science from Xi'an Jiaotong University, Xian, China, in 2009. He is currently a Professor with the Department of Information Engineering, Xijing University, Xi'an. His current research interests include artificial intelligence, intelligent agriculture, and machine vision.

RUI ZHU received the M.Sc. degree in electronic engineering from the PLA University of Science and Technology, Nanjing, China, in 2005, and the Ph.D. degree in electronic engineering from Tsinghua University, Beijing, China, in 2014. He is currently an Assistant Professor with the Information Engineering School, Xijing University, Xi'an, China. He is the author of more than 40 articles. His research interests include green communication, cognitive radio networks, and wireless resource allocation.